

High energy Rydberg and ion-pair states, state mixing and excitation dynamics of HI

Arnar Hafliðason, Meng-Xu Jiang and Ágúst Kvaran*

Science Institute, University of Iceland, Dunhagi 3, 107 Reykjavík, Iceland.

Supplementary material

Content:	pages:
Fig. S1: Overall MPI spectra of HI for $2h\nu = 74\,000 - 75\,000\text{ cm}^{-1}$, HI^+ , I^+ , H^+	2
Fig. S2 a-d): REMPI spectra of the $\text{V}^1\Sigma^+(\Omega = 0^+; v' = m + i)$; $i = 16 - 19$ ion-pair states of HI	3 - 6
Fig. S3 a-f): REMPI spectra of the $\text{j}^3\Sigma^-(\Omega = 0^+; v' = 1)$ and $\text{N}^1\Pi(\Omega = 1; v' = 2)$ Rydberg states of HI	7 - 9
Fig. S4: Simulation of the $\text{j}(1) \leftrightarrow \text{V}(m+19)$ system.....	10
Fig. S5 a-c): Effects of state interaction: Reduced term plots / $E_{J'} - E_{J'}^0$ vs. J' ,	
a) - for $\text{j}(1)$, $\text{V}(m+19)$ and $\text{N}(2)$; $E_{J'}^0$ derived by deperturbation analysis for 2 state interactions ($\text{j}(1) \leftrightarrow \text{V}(m+19)$ and $\text{N}(2) \leftrightarrow \text{V}(m+19)$).....	10
b) - for $\text{j}(1)$, $\text{V}(m+19)$ and $\text{N}(2)$; $E_{J'}^0$ derived by deperturbation analysis for 3 state interactions ($\text{j}(1) \leftrightarrow \text{V}(m+19)$ and $\text{N}(2) \leftrightarrow \text{V}(m+19)$).....	11
c) - for $\text{V}(m+16) - \text{V}(m+19)$	11
Fig. S6: Energy level diagram showing rotational energy levels for the $\text{j}(1)$, $\text{V}(m+19)$ and $\text{N}(2)$ states and level-to-level interactions.....	12
Fig. S7 a-c): Relative ion intensities for the $\text{j}(1)$ and $\text{V}(m+19)$ state spectra	12 - 14
Fig. S8 Schematic energy diagram for excitation processes.....	14
Tables S1: (a – c): Rotational lines of the ion-pair ($\text{V}(m + i)$; $i = 16 - 19$) and Rydberg ($\text{j}(1)$, $\text{N}(2)$) state spectra	15 - 16
Tables S2: Hamiltonian matrices used for deperturbation calculations.....	16
Tables S3: (a – c): Band origins (v^0) and rotational parameters (B' , D') for the ion-pair and Rydberg states of HI derived from measurements and deperturbed analysis	17 - 18
Tables S4: State interactions: Parameters derived from line-shift analysis for (a) –the $\text{j}(1)$ vs. $\text{V}(m + 19)$; homogenous interaction ($\Delta\Omega = 0$) and (b) –the $\text{N}(2)$ vs. $\text{V}(m + 19)$; heterogenous interaction ($\Delta\Omega \neq 0$).....	19
References	20

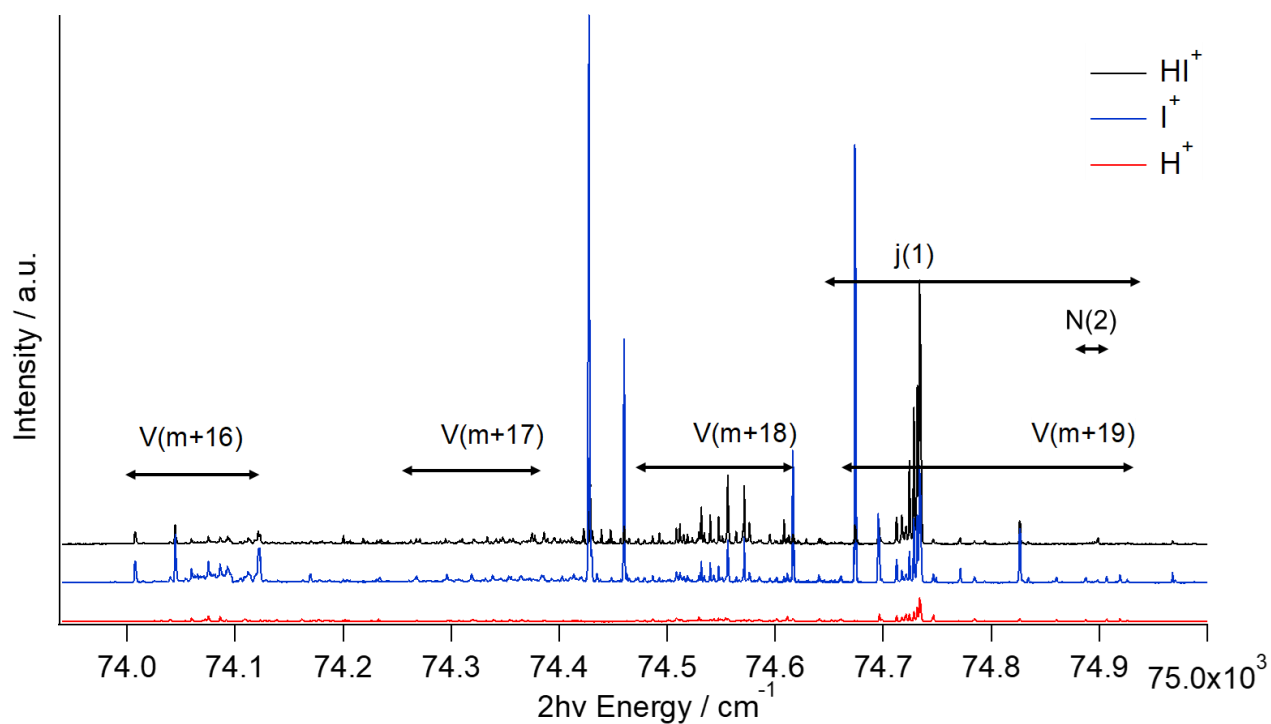


Fig. S1 Overall REMPI spectra of the ions H^+ (red), I^+ (blue) and HI^+ (black) for the two-photon ($2h\nu$) excitation region of $73\,980 - 75\,000 \text{ cm}^{-1}$. States identified are indicated. Horizontal double arrows cover the energy region of individual spectra.

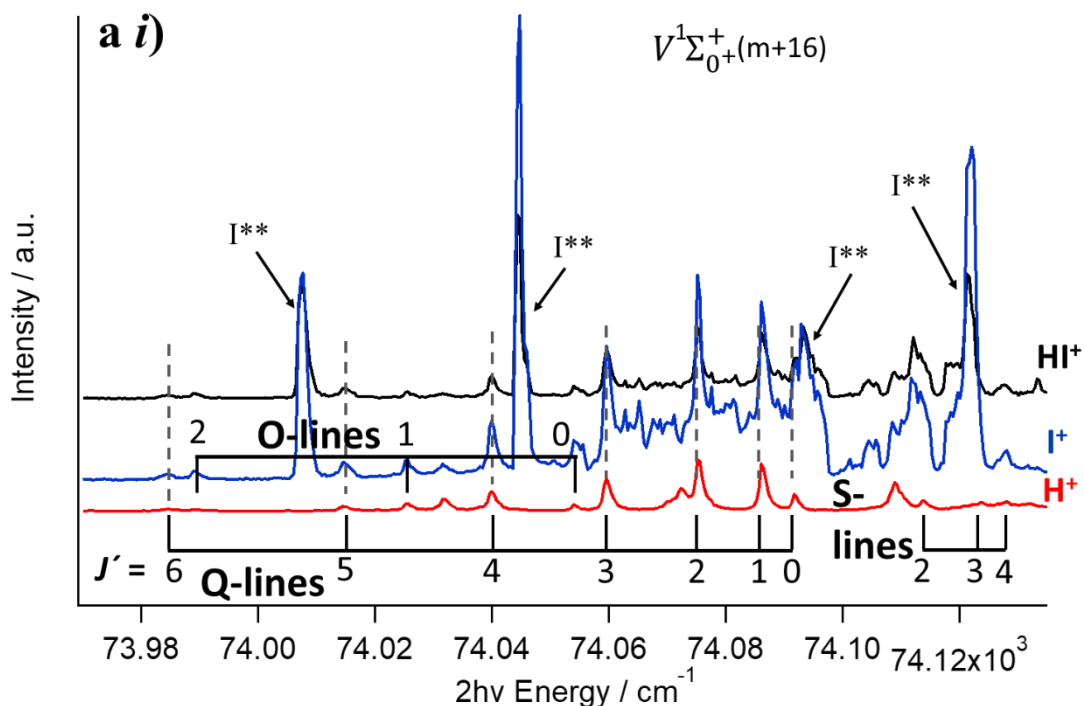


Fig. S2 a i) REMPI spectra of H⁺(red), I⁺(blue) and HI⁺(black) for the two-photon (2hv) excitation region of 73 970 – 74 125 cm⁻¹. Rotational lines are labeled (J') and indicated by vertical lines for the V(m+16) ion-pair state spectra, for the O, Q and S line series. I** indicate atomic lines.

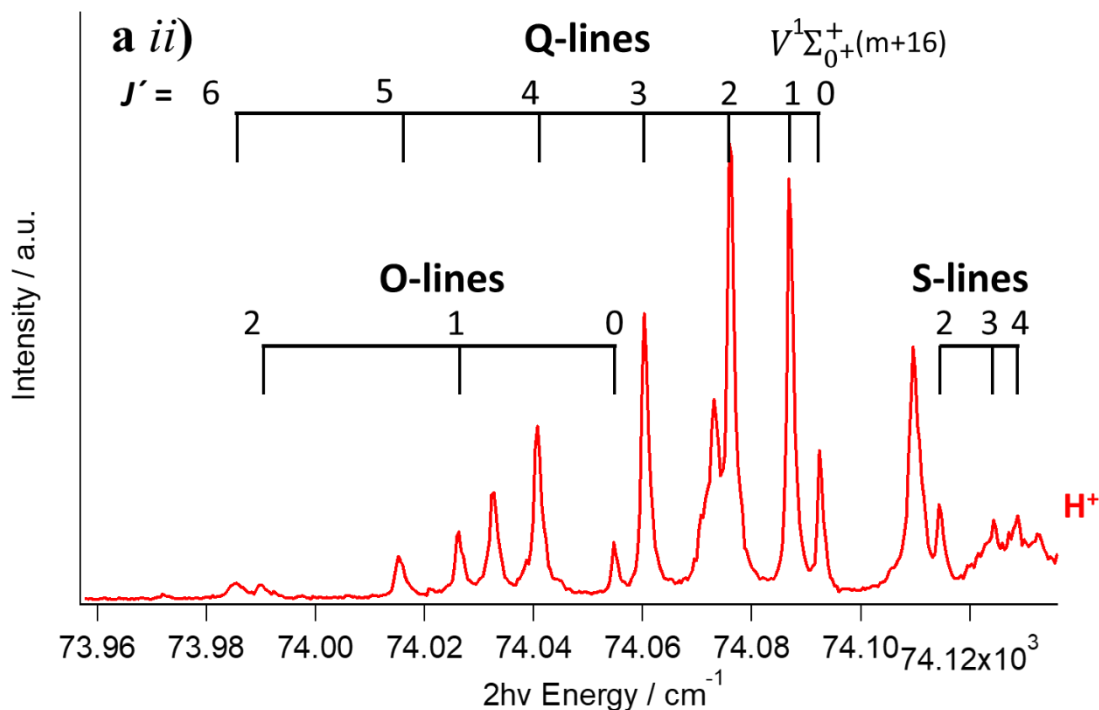


Fig. S2 a ii) REMPI spectrum of H⁺(red) for the two-photon (2hv) excitation region of 73 960 – 74 125 cm⁻¹. Rotational lines are labeled (J') and indicated by vertical lines for the V(m+16) ion-pair state spectrum, for the O, Q and S line series.

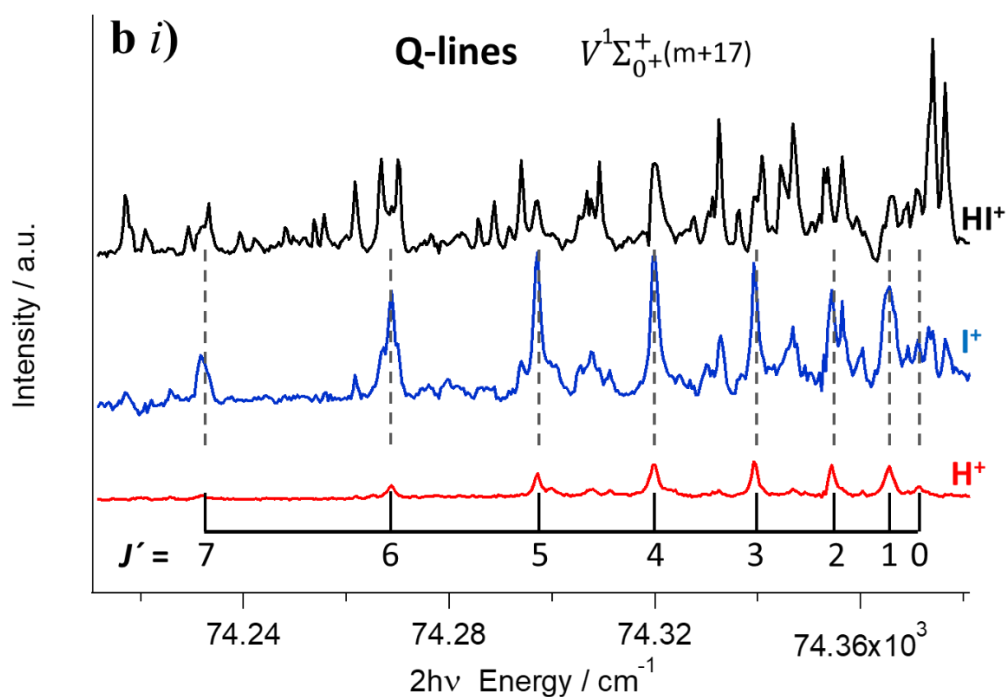


Fig. S2 b i) REMPI spectra of H⁺(red), I⁺(blue) and HI⁺(black) for the two-photon (2hv) excitation region of 74 215 – 74 380 cm⁻¹. Rotational Q-lines are labeled (J') and indicated by vertical lines for the V(m+17) ion-pair state spectra.

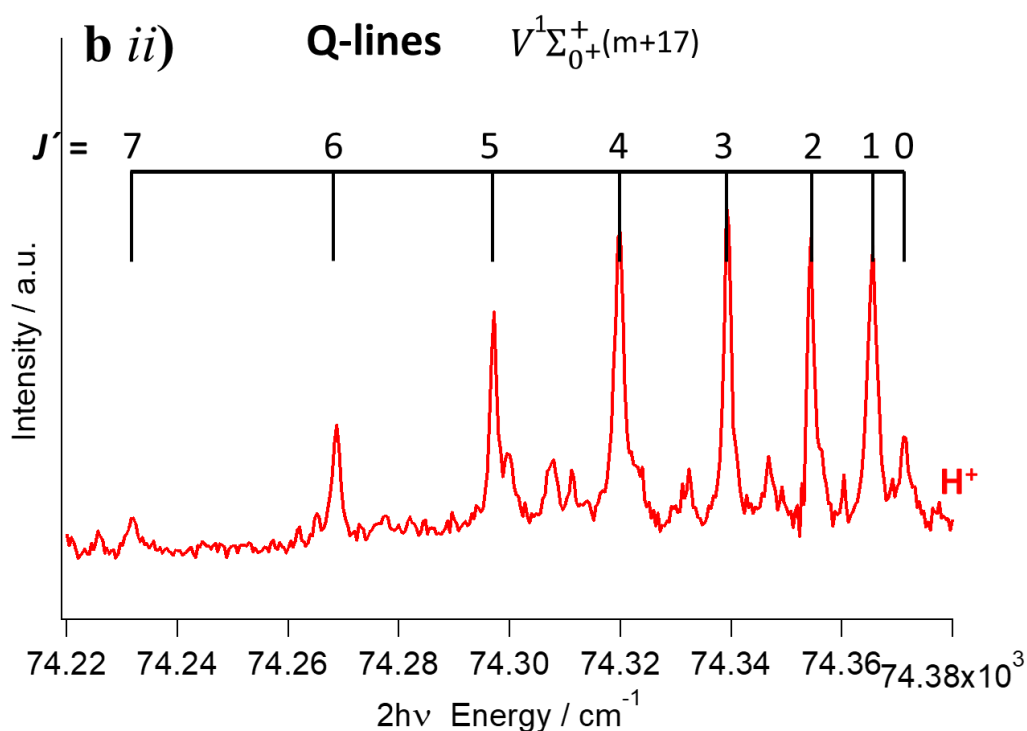


Fig. S2 b ii) REMPI spectrum of H⁺(red) for the two-photon (2hv) excitation region of 74 220 – 74 380 cm⁻¹. Rotational Q-lines are labeled (J') and indicated by vertical lines for the V(m+17) ion-pair state spectrum.

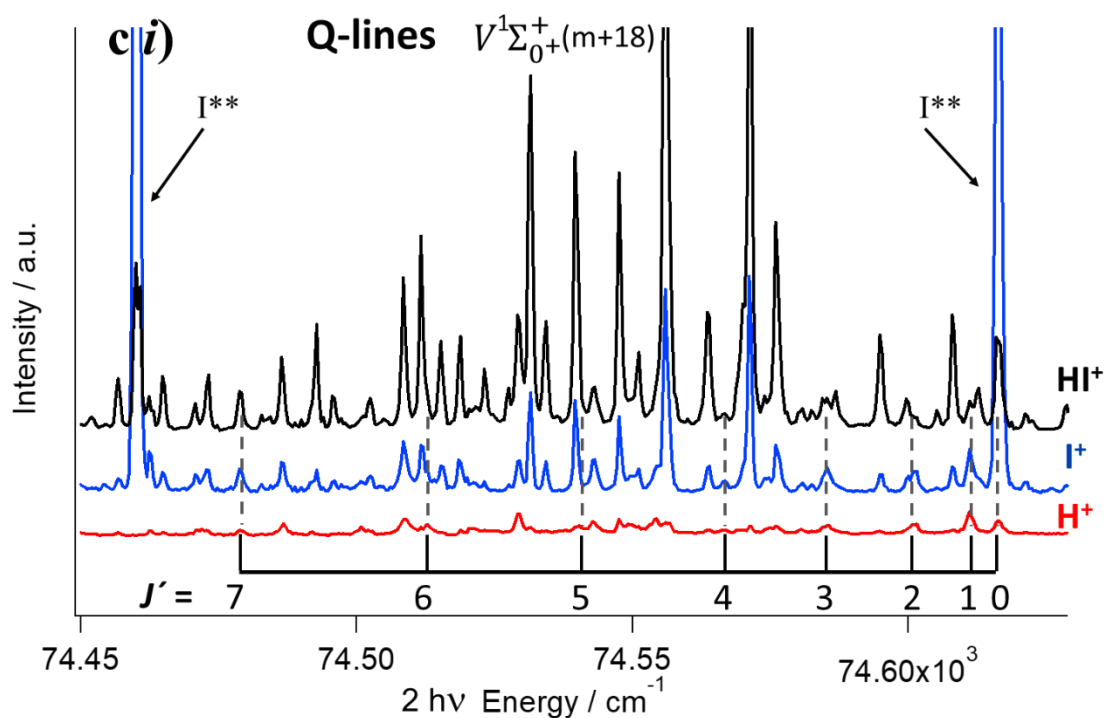


Fig. S2 c i) REMPI spectra of H^+ (red), I^+ (blue) and HI^+ (black) for the two-photon (2hv) excitation region of $74\,450 - 74\,650 \text{ cm}^{-1}$. Rotational Q-lines are labeled (J') and indicated by vertical lines for the $V(m+18)$ ion-pair state spectra. I^{**} indicate atomic lines.

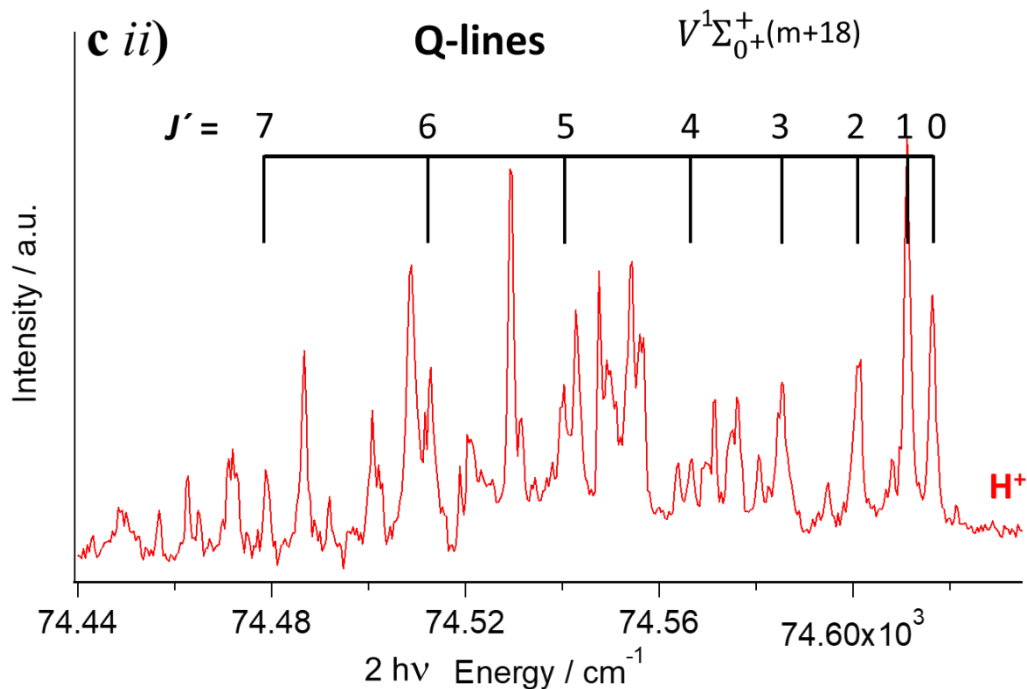


Fig. S2 c ii) REMPI spectrum of H^+ (red) for the two-photon (2hv) excitation region of $74\,220 - 74\,380 \text{ cm}^{-1}$. Rotational Q-lines are labeled (J') and indicated by vertical lines for the $V(m+18)$ ion-pair state spectrum.

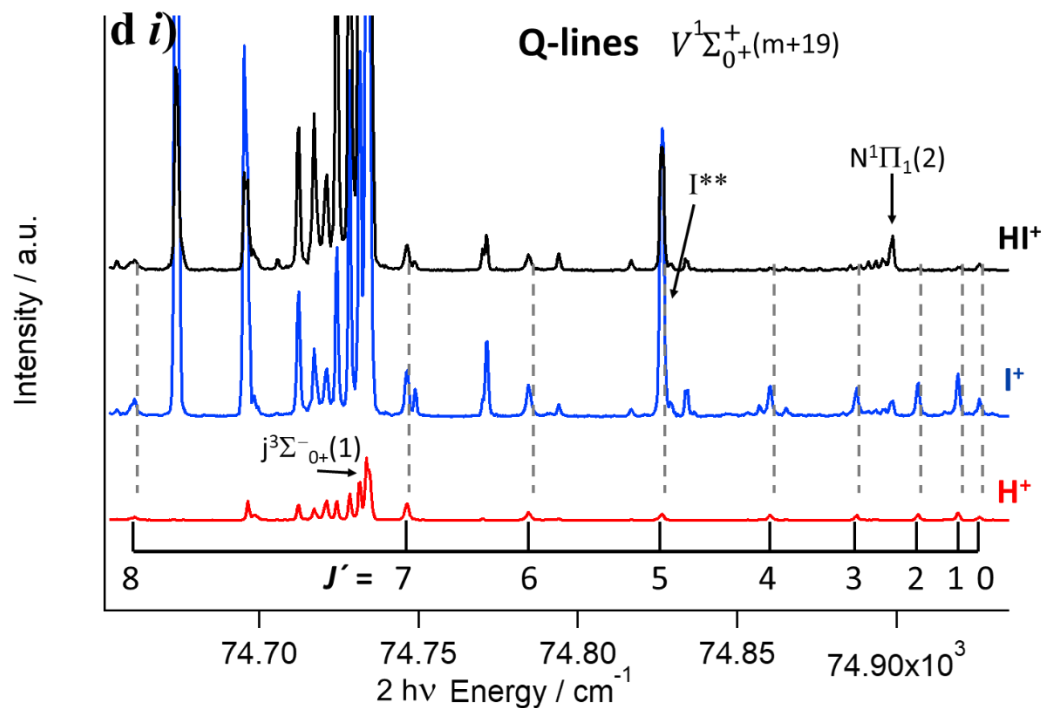


Fig. S2 d i) REMPI spectra of H⁺(red), I⁺(blue) and HI⁺(black) for the two-photon (2hv) excitation region of 74 650 – 74 950 cm⁻¹. Rotational Q-lines are labeled (J') and indicated by vertical lines for the V(m+19) ion-pair state spectra. I** indicates a atomic line. Spectra of the j³Σ₀⁻(1) and N¹Π₁(2) Rydberg states are observed at 74 735 cm⁻¹ and 74 900 cm⁻¹, respectively.

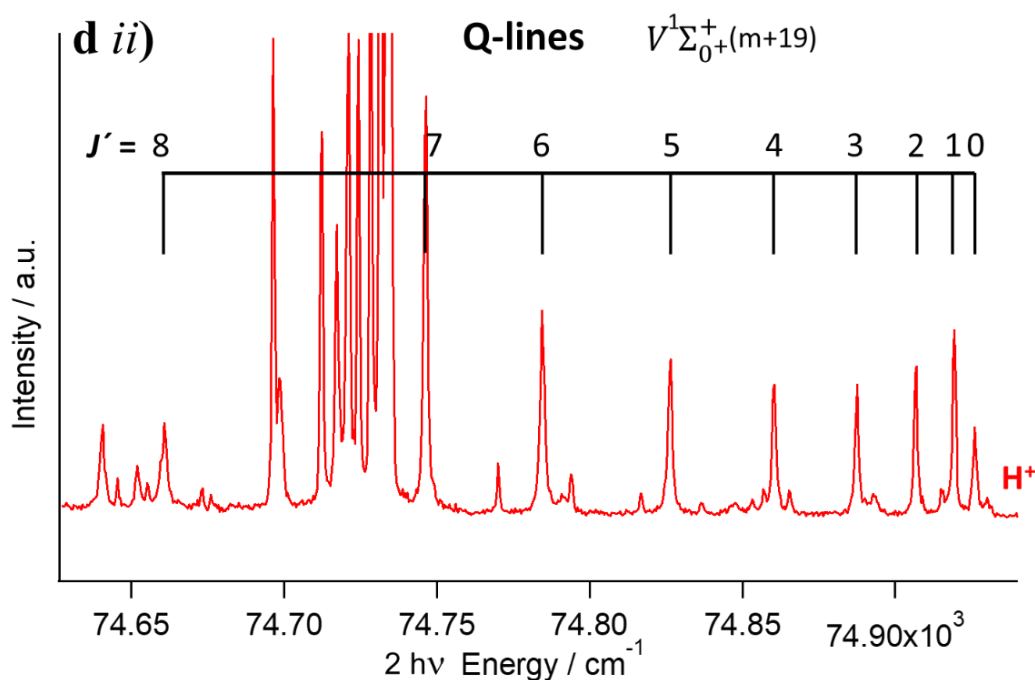


Fig. S2 d ii) REMPI spectrum of H⁺(red) for the two-photon (2hv) excitation region of 74 640 – 74 940 cm⁻¹. Rotational Q-lines are labeled (J') and indicated by vertical lines for the V(m+19) ion-pair state spectrum.

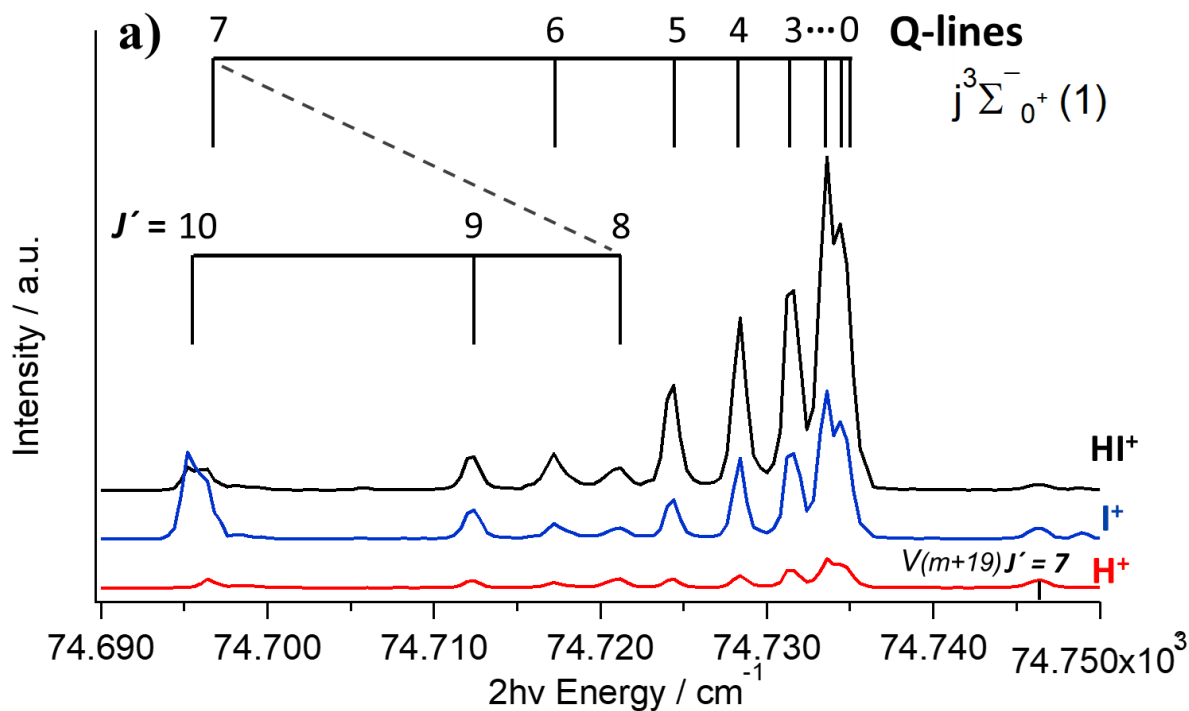


Fig. S3 a) REMPI spectra of H^+ (red), I^+ (blue) and HI^+ (black) for the two-photon ($2h\nu$) excitation region of $74\,690 - 74\,750\text{ cm}^{-1}$. Rotational Q-lines are labeled (J') and indicated by vertical lines for the $j(1)$ Rydberg state spectra. The $J'=7$, Q line, for $V(m+19)$ is to be seen at $74\,747\text{ cm}^{-1}$.

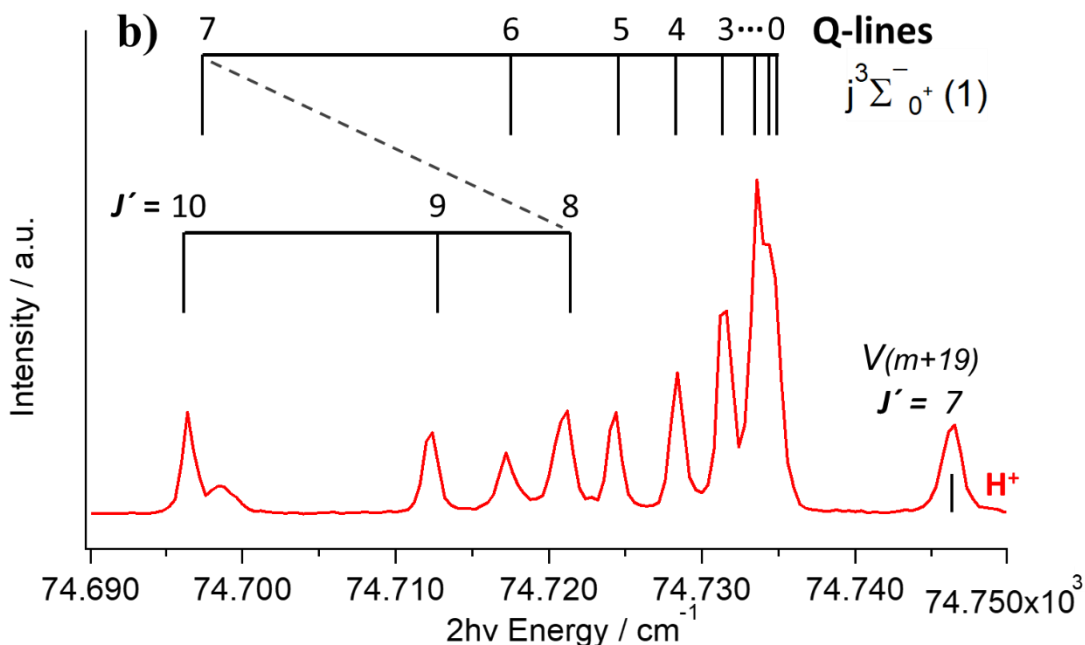


Fig. S3 b) REMPI spectrum of H^+ (red) for the two-photon ($2h\nu$) excitation region of $74\,690 - 74\,750\text{ cm}^{-1}$. Rotational Q-lines are labeled (J') and indicated by vertical lines for the $j(1)$ Rydberg state spectrum. The $J'=7$, Q line, for $V(m+19)$ is to be seen at $74\,747\text{ cm}^{-1}$.

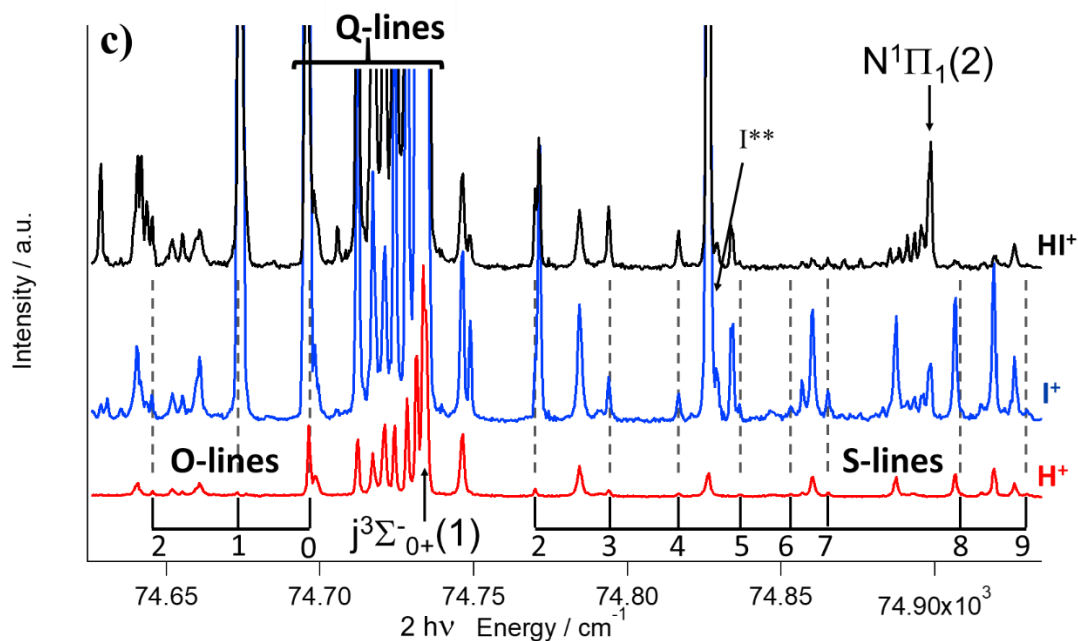


Fig. S3 c) REMPI spectra of H⁺(red), I⁺(blue) and HI⁺(black) for the two-photon (2hv) excitation region of 74 690 – 74 750 cm⁻¹. Rotational O- and S-lines are labeled (*J'*) and indicated by vertical lines for the j(1) Rydberg state spectra. I** indicates an iodine atomic line. Spectrum of the Rydberg state N¹Π₁(2) is at 74 900 cm⁻¹.

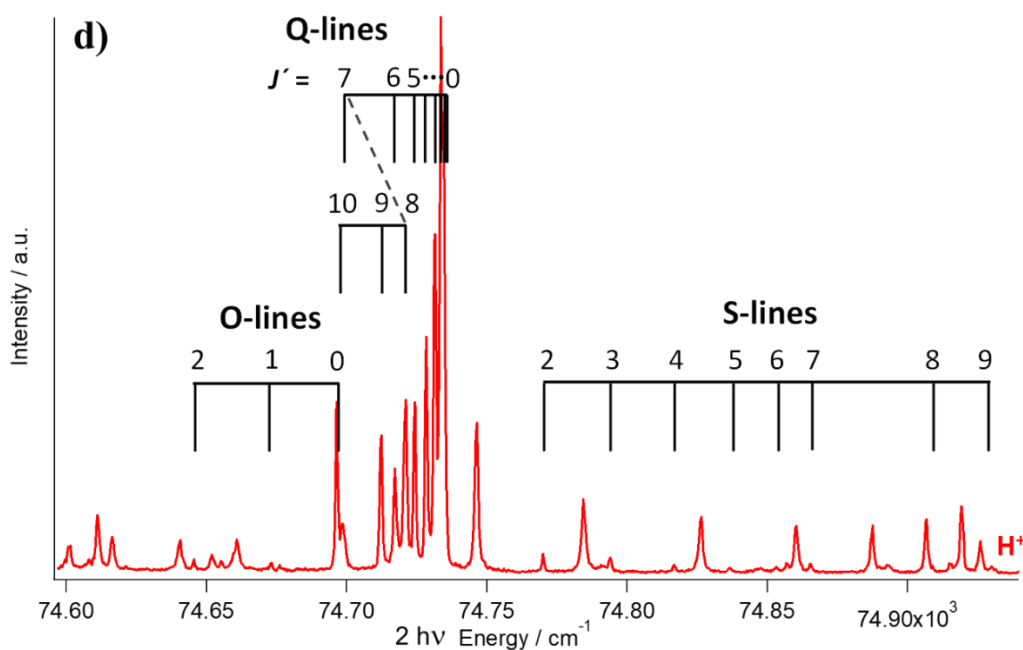


Fig. S3 d) REMPI spectrum of H⁺(red) for the two-photon (2hv) excitation region of 74 600 – 74 950 cm⁻¹. Rotational O-, Q- and S-lines are labeled (*J'*) and indicated by vertical lines for the j(1) Rydberg state spectrum.

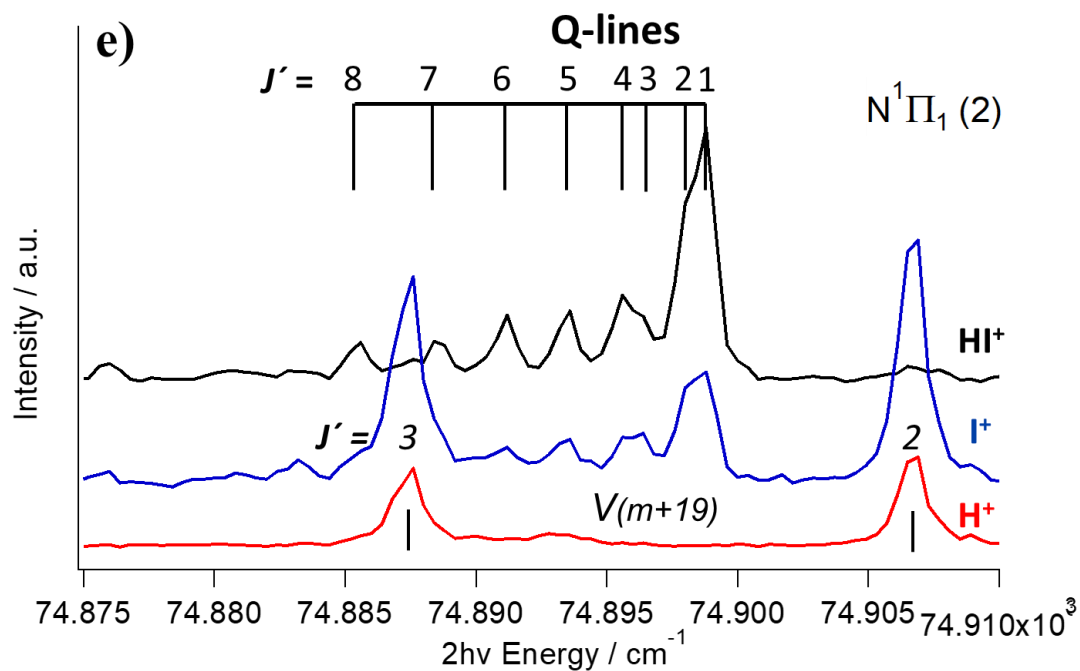


Fig. S3 e) REMPI spectra of H⁺(red), I⁺(blue) and HI⁺(black) for the two-photon (2hv) excitation region of 74 690 – 74 750 cm⁻¹. Rotational Q-lines are labeled (*J'*) and indicated by vertical lines for the N(2) Rydberg state spectra. *J'*=2 and 3, Q lines, for V(m+19) are also labeled.

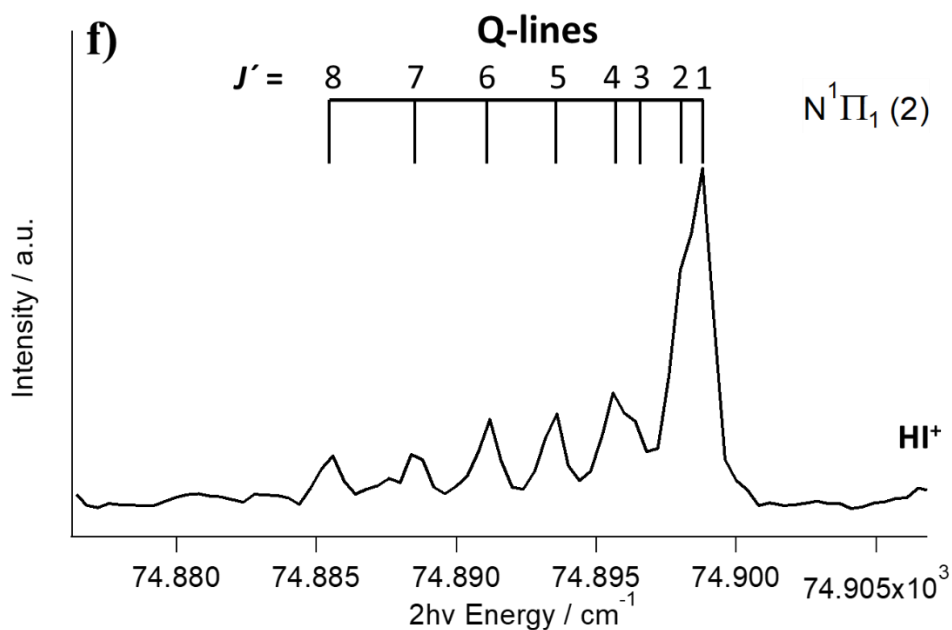


Fig. S3 f) REMPI spectra of HI⁺(black) for the two-photon (2hv) excitation region of 74 875 – 74 905 cm⁻¹. Rotational Q-lines are labeled (*J'*) and indicated by vertical lines for the N(2) Rydberg state spectrum.

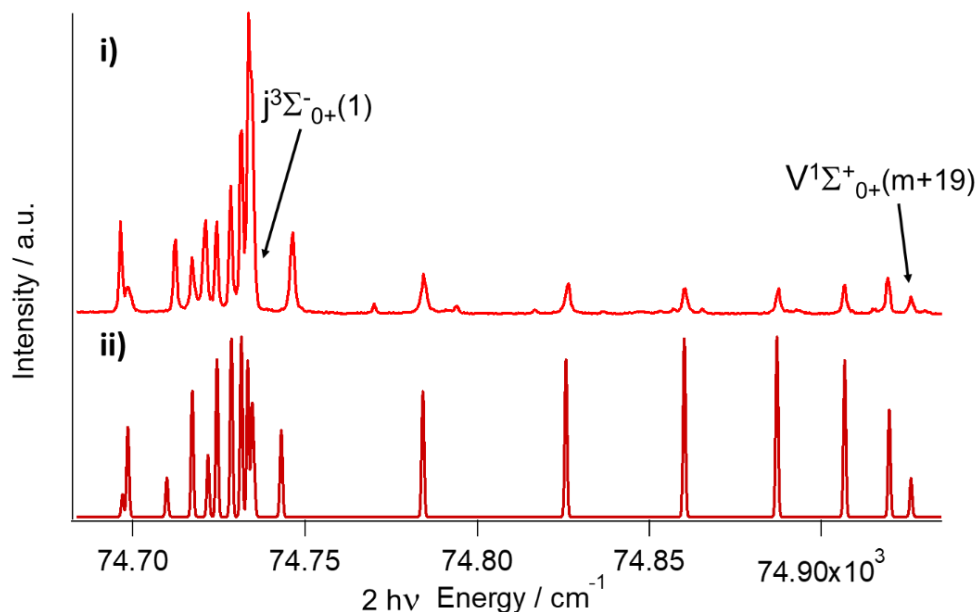


Fig. S4 Simulation: Comparison of the experimental spectra for $j(1)$ and $V(m+19)$ and corresponding calculated two-photon absorption spectra. Black arrows indicate the band origin for the two states. **i)** Two-photon REMPI spectrum of HI for the H^+ ion. **ii)** Calculated two-photon absorption spectrum¹. (See Fig. S2 d ii) and S3 b) for assignment)

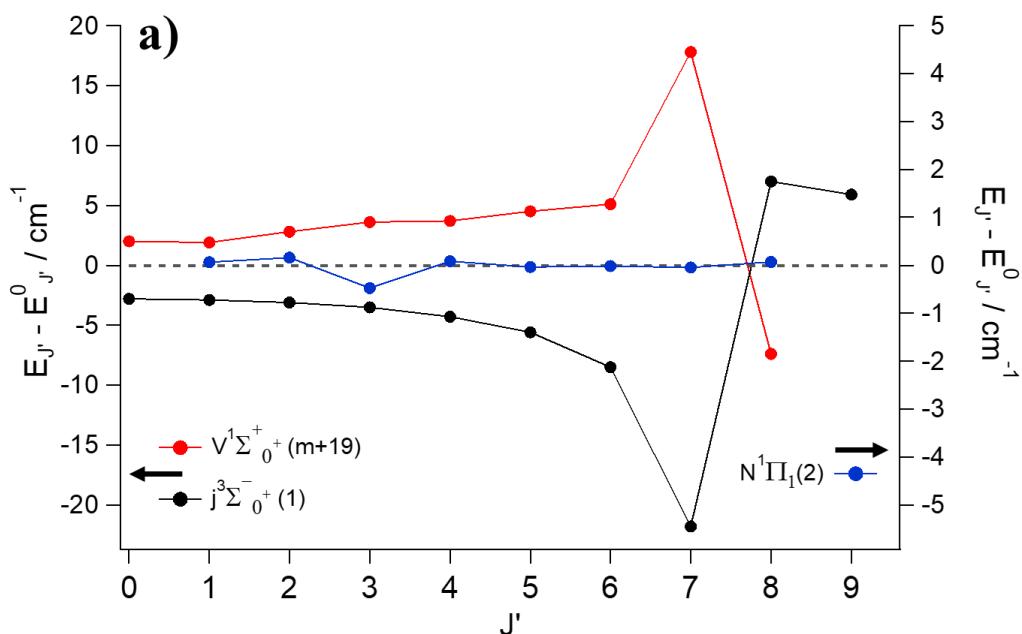


Fig. S5 a) Reduced term value plots for the $V(m+19)$, $j(1)$ and $N(2)$ states: Deperturbed energy level values subtracted from experimental energy level values. Homogenous coupling between the $j(1)$ and $V(m+19)$ states appears as gradual changes in the energy differences for $J' = 0 - 6$ (i.e. non-degenerate interaction), whereas a near-degenerate interaction is seen for $J' = 7 - 8$. Small deviations of the energies from deperturbed values were observed for $J' = 2$ and $J' = 3$ for $N(2)$ (and $V(m+19)$) (near-degenerate interactions) due to heterogenous coupling. Deperturbation calculations were performed by assuming independent **two-state interactions**.

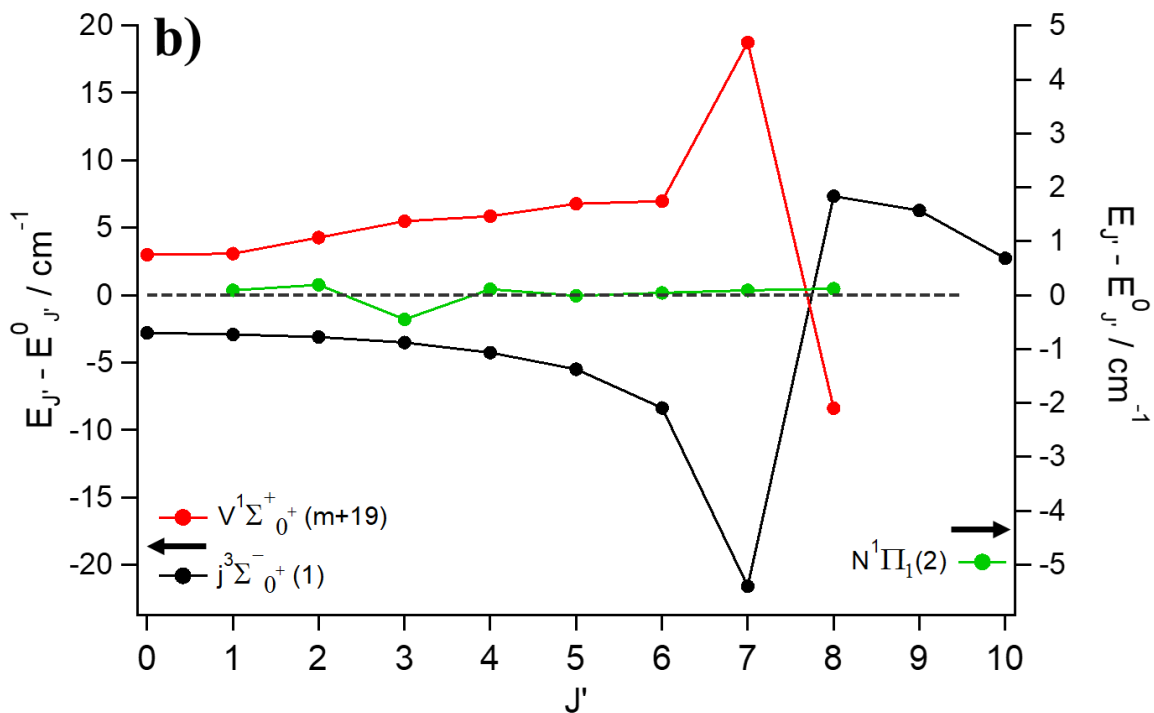


Fig. S5 b) Reduced term value plots for the V(m+19), j(1) and N(2) states: Deperturbed energy level values subtracted from experimental energy level values. Homogenous coupling between the j(1) and V(m+19) states appears as gradual changes in the energy differences for $J' = 0 - 6$ (i.e. non-degenerate interaction), whereas a near-degenerate interaction is seen for $J' = 7 - 8$. Small deviations of the energies from deperturbed values were observed for $J' = 2$ and $J' = 3$ for N(2) (and V(m+19)) (near-degenerate interactions) due to heterogenous coupling. Deperturbation calculations were performed by assuming **three-state interaction**.

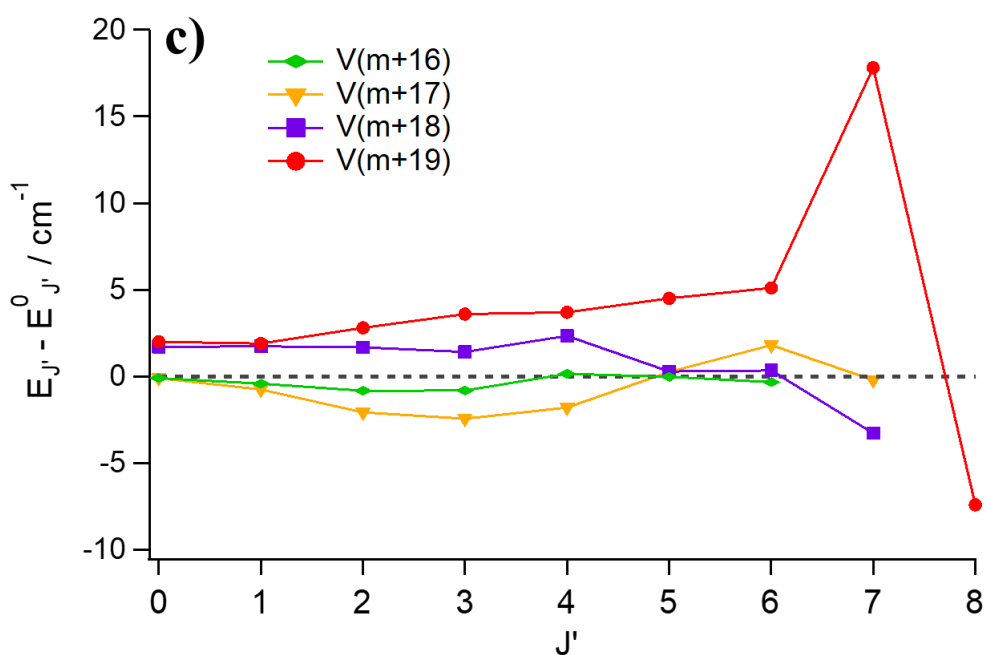


Fig. S5 c) Reduced term value plots for V(m + i); $i = 16 - 19$. All states show indications of interaction with neighboring Rydberg states.

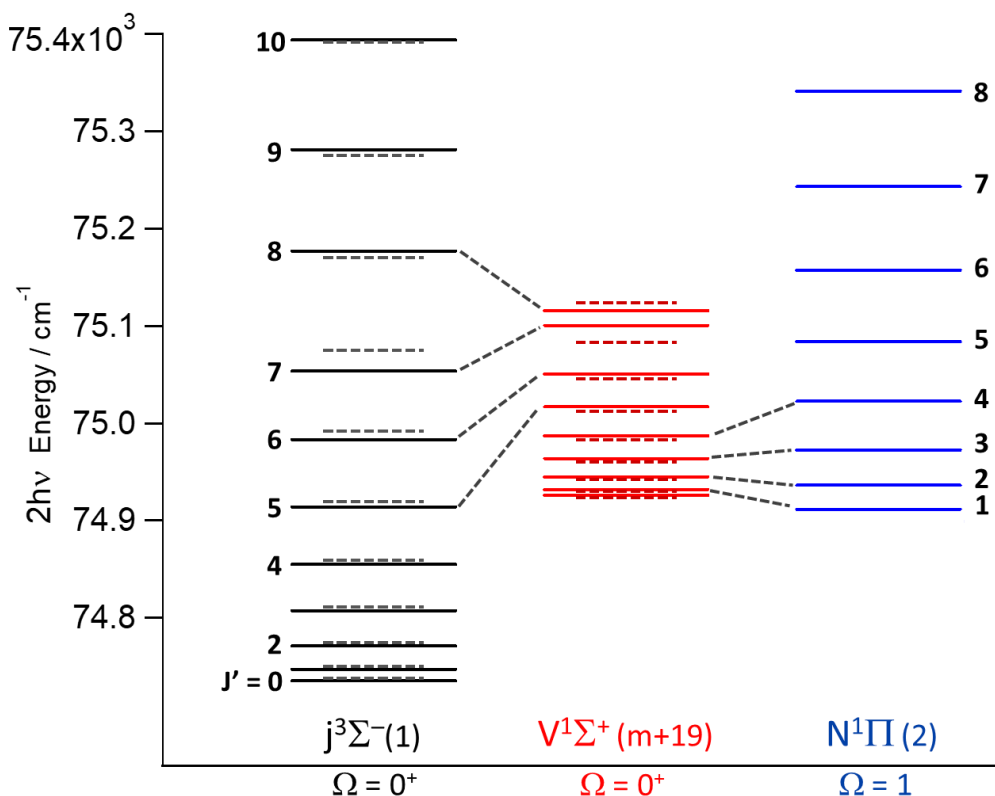


Fig. S6 Rotational energy levels derived from spectral peak positions for states $j(1)$, $V(m+19)$ and $N(2)$ (solid lines). Energy levels derived from deperturbation analysis (broken lines). Close to degenerate interactions are indicated by broken leaned lines connecting energy levels of same J' values.

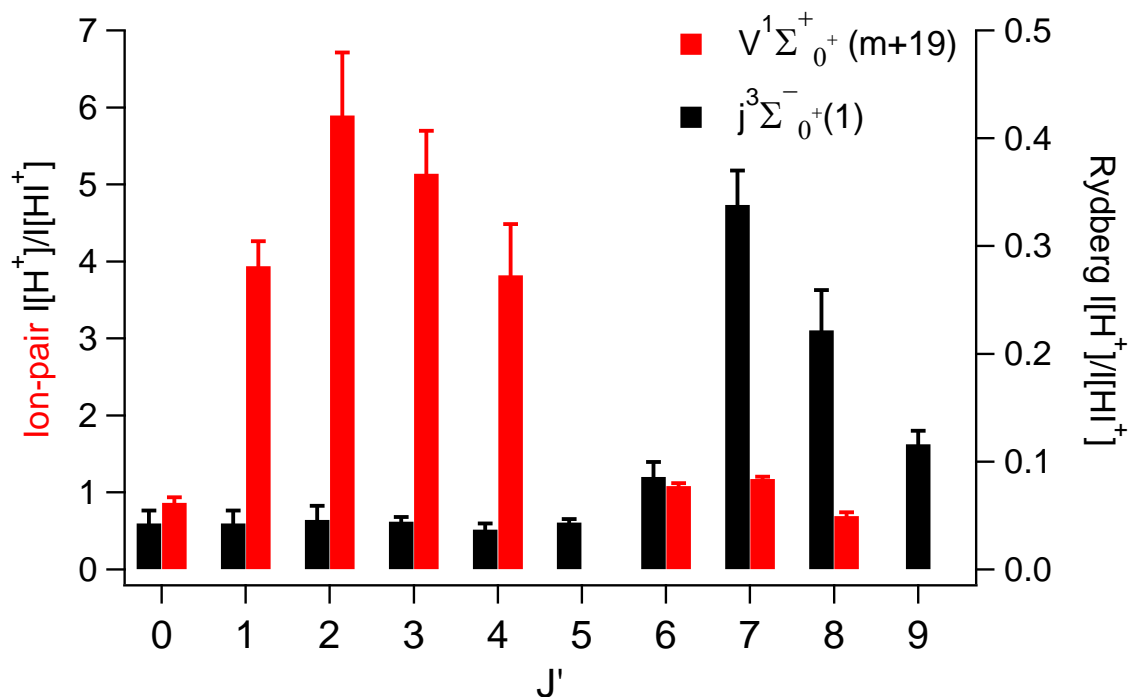


Fig. S7 a) Relative ion-signal intensities ($I(H^+)/I(HI^+)$) vs. J' derived from the Q-rotational lines for the $j(1)$ and $V(m + 19)$ spectra.

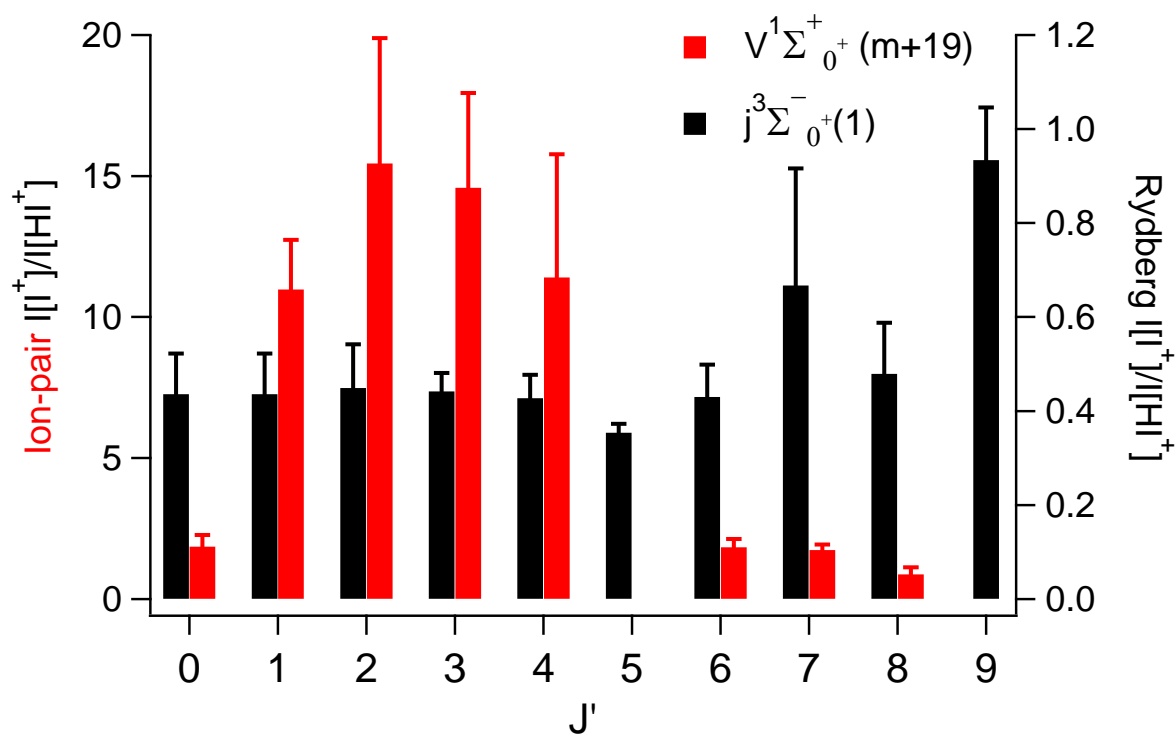


Fig. S7 b) Relative ion-signal intensities $I(I^+)/I(HI^+)$ vs. J' derived from the Q-rotational lines for the $j(1)$ and $V(m + 19)$ spectra.

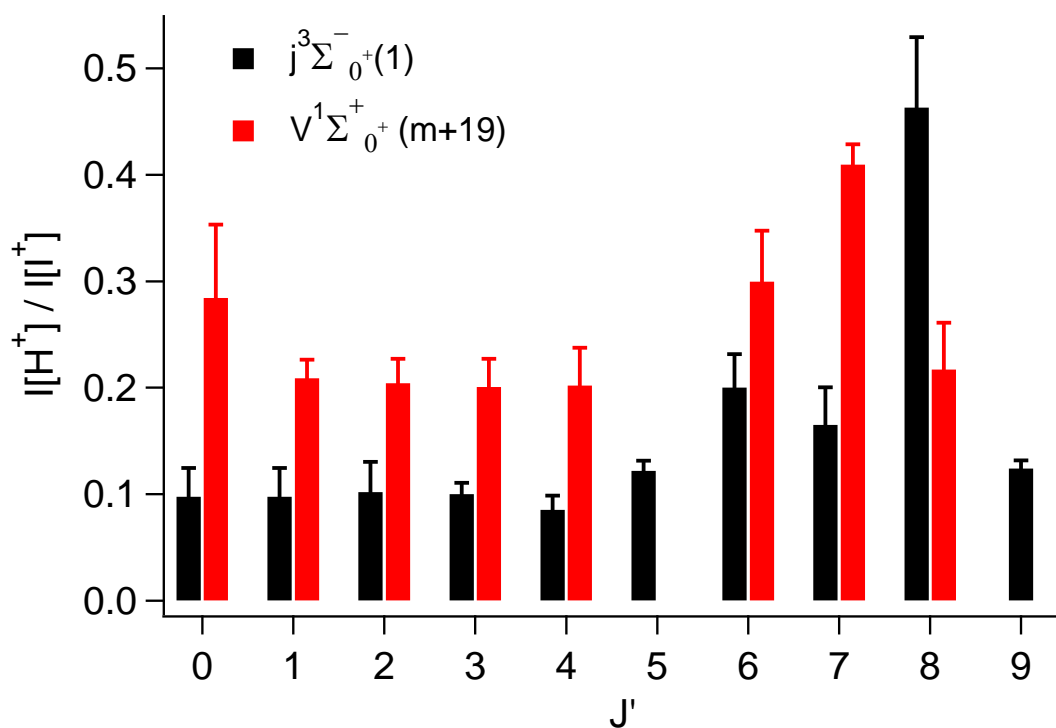


Fig. S7 c) Relative ion-signal intensities $I(H^+)/I(I^+)$ vs. J' derived from the Q-rotational lines for the $j(1)$ and $V(m + 19)$ spectra.

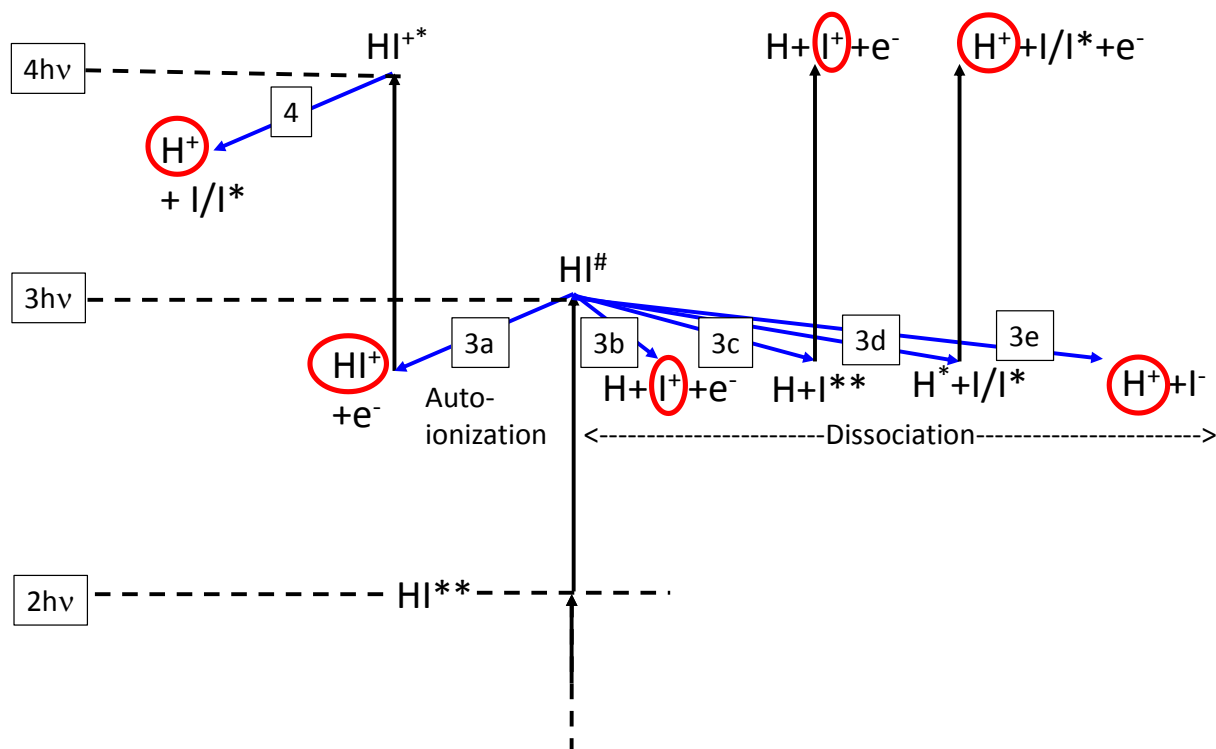


Fig. S8 Schematic energy diagram for excitation processes of HI in the two-photon energy region of $74\,000 - 75\,000\text{ cm}^{-1}$. Vertical black arrows denote photon absorption. Blue arrows denote fragmentation (autoionization (3a) and dissociation (3b,3c,3d,3e,4)) processes. The numbers in inside boxes are the number of photons absorbed prior to the fragmentation processes. HI^{**} , and $\text{HI}^\#$ are resonant and superexcited neutral molecular states, respectively. HI^+ and HI^{+*} are ground and excited ion states, respectively. I, I^* and I^{**} are ground, spin-orbit excited and Rydberg states of iodine atoms, respectively. Ions detected are highlighted by red circles.

Table S1. Rotational lines for HI due to two-photon resonant transitions to four vibrational levels ($v' = m + i$); $i = 16, 17, 18$ and 19 of the $V^1\Sigma^+$ ion-pair state and to the $j^3\Sigma^-$ ($v' = 1$) and $N^1\Pi(v' = 2)$ Rydberg states. $J = J'$

Table 1a. Wavenumbers for measured REMPI transitions in HI for $V^1\Sigma^+ \leftarrow\leftarrow X^1\Sigma^+ (m + i, 0)$

J	i:	16		17	18	19	
		O(J)	Q(J)	S(J)	Q(J)	Q(J)	Q(J)
0		74054.0	74091.7		74371.2	74616.4	74926.0
1		74025.2	74086.1		74365.6	74611.2	74919.3
2		73988.8	74075.2	74113.7	74354.4	74600.8	74906.9
3			74059.6	74123.7	74339.2	74585.3	74887.6
4			74040.0	74128.1	74320.0	74566.4	74860.4
5			74014.5		74297.2	74540.4	74826.5
6			73984.4		74268.8	74512.9	74784.4
7					74231.7	74478.8	74746.1
8							74660.8

Table 1b. Wavenumbers for measured REMPI transitions in HI for $j^3\Sigma^-_{-0+} \leftarrow\leftarrow X^1\Sigma^+ (1, 0)$

J	O (J)	P (J)	Q (J)	R (J)	S (J)
0	74698.8		74735.2		
1	74672.9		74734.6		
2	74645.6		74733.7		74794.0
3			74731.6		74770.4
4			74728.4		74836.5
5			74724.1		74816.8
6			74717.2		74865.2
7			74699.2		74853.2
8			74721.2		74930.0
9			74712.0		74908.9
10			74698.4		

Table 1c. Wavenumbers for measured REMPI transitions in HI for $N^1\Pi_1 \leftarrow\leftarrow X^1\Sigma^+ (2,0)$

J	O (J)	P (J)	Q (J)	R (J)	S (J)
0					
1			74898.8		
2			74898.2		
3			74896.5		
4			74895.6		
5			74893.6		
6			74891.3		
7			74888.5		
8			74885.4		

Table S2. Deperturbation analysis

Hamiltonian matrices, used to derive interaction strengths (W , W') and zero order state energies (E^0) by diagonalization for **a)** two- and **b)** three-state interactions. W is an interaction strength for homogenous interaction and W' stands for heterogenous interaction strength. States of concern are $E_1^0=V(m+19)$, $E_2^0=j(1)$ and $E_3^0=N(2)$:

a) Two state interaction matrices:

$$\begin{array}{cc} E_1^0 & W \\ W & E_2^0 \end{array} \quad \text{and} \quad \begin{array}{cc} E_1^0 & W' \\ W' & E_3^0 \end{array}$$

b) Three state interaction matrix:

$$\begin{array}{ccc} E_1^0 & W & W' \\ W & E_2^0 & 0 \\ W' & 0 & E_3^0 \end{array}$$

Table S3. Band origin (ν^0) and rotational constants (B' and D') attained by traditional line fitting and simulation / deperturbation.

a) $V^1\Sigma^+$ ion-pair vibrational states; Fit analysis

State	ν'	ν^0/cm^{-1}		B'/cm^{-1}		$D' \times 10^3/\text{cm}^{-1}$		$H' \times 10^6/\text{cm}^{-1}$
		Our	Others'	Our	Others'	Our	Others'	
$V^1\Sigma^+$	16	74 091.0	74 090 ^a	3.714	3.724 ^a	2.262	0.588 ^a	0
$V^1\Sigma^+$	17	74 372.0		3.896		0.418		0
$V^1\Sigma^+$	18	74 615.4		3.763		3.670		0
$V^1\Sigma^+$	19	74 926.0		3.177		7.650		1.50

a. *Ginter et al. (assigned as $V(m+14)$)²*

b) Rydberg states; Fit analysis

State	ν'	ν^0		B'/cm^{-1}		$D' \times 10^3/\text{cm}^{-1}$		$H' \times 10^6/\text{cm}^{-1}$
		Our	Others'	Our	Others'	Our	Others'	
$j^3\Sigma^-$	1	74 735.2		6.053		1.115		2.40
$N^1\Pi_1$	2	74 899.2		6.1605		0.390		0

c) Deperturbation analysis

- i.** Values derived by assuming two state interactions at a time: Homogenous coupling between $j(1) \leftrightarrow V(m+19)$ and heterogenous coupling between $N(2) \leftrightarrow V(m+19)$.

State	ν'	ν^0/cm^{-1}		B^0/cm^{-1}		$D^0 \times 10^3/\text{cm}^{-1}$		Ω
		Our	\pm	Our	\pm	Our	\pm	
$V^1\Sigma^+$	19	74 924.0	1	3.049	0.048	3.83	0.86	0+
$j^3\Sigma^-$	1	74 738.0	1	6.102	0.031	1.48	0.28	0+
$N^1\Pi_1$	2	74899.1	1	6.171	0.015	0.62	0.26	1

- ii. Values derived by assuming three state interactions: $j(1) \leftrightarrow V(m+19) \leftrightarrow N(2)$ for homogenous coupling between $j(1) \leftrightarrow V(m+19)$ and heterogenous coupling between $V(m+19) \leftrightarrow N(2)$.

State	v'	v^0/cm^{-1}		B^0/cm^{-1}		$D^0 \times 10^3/\text{cm}^{-1}$		Ω
		Our	\pm	Our	\pm	Our	\pm	
$V^1 \Sigma^+$	19	74 923	3	2.958	0.123	2.17	1.46	0+
$j^3 \Sigma^-$	1	74 738	1	6.101	0.021	1.51	0.20	0+
$N^1 \Pi_1$	2	74899	3	6.171	0.205	0.54	3.01	1

Table S4. Rydberg to ion-pair state interactions.

- a) **j(1) vs. V(m + 19)** / Homogeneous ($\Delta\Omega = 0$) coupling: Parameters derived from deperturbation analysis of the j(1) Rydberg state (state labelled 1 in table)) and V(m + 19) ion-pair state (state labelled 2 in table) spectra. J' level proximity ($\Delta E_{J'} = E_{J'}(1) - E_{J'}(2) / \text{cm}^{-1}$), interaction strength (W_{12} / cm^{-1}) and fractional state mixing (c_1^2, c_2^2).

J'	$\Delta E_{J'}$	W_{12}	c_1^2	c_2^2
0	-190.8	22.3	0.986	0.014
1	-184.7	22.3	0.985	0.015
2	-173.5	22.3	0.983	0.017
3	-156.2	22.3	0.979	0.021
4	-132.0	22.3	0.971	0.029
5	-102.4	22.3	0.950	0.050
6	-67.2	22.3	0.875	0.125
7	-47.3	22.3	0.669	0.331
8	60.4	22.3	0.838	0.162

- b) **N(2) vs. V(m + 19)** / Heterogeneous ($\Delta\Omega \neq 0$) coupling: Parameters derived from deperturbation analysis of the N(2) Rydberg state (state labelled 1)) and V(m + 19) ion-pair state (state labelled 2) spectra. J' level proximity ($\Delta E_{J'} = E_{J'}(1) - E_{J'}(2) / \text{cm}^{-1}$), interaction strength ($W_{12} = 0.75(J'(J'+1))^{1/2} / \text{cm}^{-1}$) and fractional state mixing (c_1^2, c_2^2).

J'	$\Delta E_{J'}$	W_{12}	c_1^2	c_2^2
1	-20.5	1.06	0.997	0.003
2	-9.0	1.84	0.953	0.047
3	8.5	2.60	0.906	0.094
4	35.2	3.35	0.991	0.009
5	67.1	4.11	0.996	0.004
6	106.9	4.86	0.998	0.002

Reference

1. C. M. Western, *PGOPHER, a Program for Simulating Rotational Structure*, C. M. Western, University of Bristol, <http://pgopher.chm.bris.ac.uk> University of Bristol 9.0.116 edn., 2003-2015.
2. D. S. Ginter, M. L. Ginter and S. G. Tilford, *J. Mol. Spectrosc.*, 1982, **92**, 40.